Contemporary Engineering Sciences, Vol. 9, 2016, no. 15, 743 - 754
HIKARI Ltd, www.m-hikari.com
http://dx.doi.org/10.12988/ces.2016.6564

A Clustering-Based Method for Brain Tumor Segmentation

Idanis Diaz Bolaño

Faculty of Engineering
Universidad del Magdalena, Santa Marta, Colombia

German Sanchez Torres

Faculty of Engineering
Universidad del Magdalena, Santa Marta, Colombia

Abstract

This work introduces a new brain tumor segmentation method based on a new criterion function for threshold selection. The method aims to accomplish some features that are desirable in medical practice such as simplicity, speed, accuracy, and independency of user inputs or parameters. Although the criterion function can be seen as an extension of Otsu's criterion, we did not assume low intra-variance for both classes, object and background. The new criterion is adapted to treat the tumor as the object to be segmented and a portion of healthy brain tissue as the background. In order to speed up the search for the thresholds, the segmentation method exploits domain knowledge by using some feature points in the histogram to bound a range of interest for searching. We evaluated the method on a set of 30 patient cases with their respective magnetic resonance images and compared the criterion function against other well-known criteria for threshold selection. The new criterion outperformed the other criteria in segmenting the complete region affected by the tumor for each patient case.

Keywords: Brain tumor segmentation, Automatic thresholding, Cluster based criterion

1 Introduction

Image segmentation provides relevant information for diagnosis, treatment planning, and monitoring of brain tumors. Usually, segmenting brain tumors entails processing Magnetic Resonance Images (MRIs) because this image modality produces detailed pictures of the brain and is not invasive. Hence, manual segmentation of brain tumors implies not only processing volumetric data, but also dealing with some characteristic problems of MRI, such as fuzzy boundaries between the region of interest and other objects in the image as well as the presence of artifacts. Figure 1 shows a brain tumor in different types of MRIs.

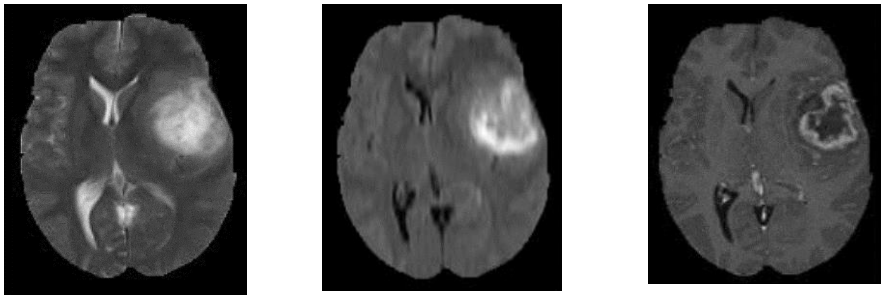

a) T2 b) Flair c) T1c

Figure 1. Brain tumor in different MRI modalities

The development of automatic segmentation methods has been of great interest. However, the medical practice still requires automatic methods with some desirable features such as simplicity, speed, operator independency, and accuracy. Most of the brain tumor segmentation methods in the literature are operator dependent, time consuming, computationally expensive, and mathematically complex to understand [9].

Thresholding is one of the most popular, simplest, and fastest techniques for image segmentation. The basic principle of this technique is to choose an intensity value that separates the image into two regions: object and background [8]. Given an intensity image $I(x, y, z)$, a threshold τ produces another image $g(x, y)$, such that:

$$g(x,y,z) = \begin{cases} 1 & If\ I(x,y,z) \geq \tau \\ 0 & Otherwise \end{cases} \quad (1)$$

The automatic selection of τ is the challenge to be solved for thresholding techniques. The methods proposed for this purpose have been classified in two categories: methods based on a criterion function and methods based on the image histogram shape. This work focuses on the first category, which may be further divided into methods based on entropy and methods based on clustering. Methods based on entropy address the problem by maximizing or minimizing an entropy

function. Pun [10] introduced, for the first time, a method based on the maximum entropy principle. Later, Kapur [4] proposed a criterion that maximizes the entropy of two classes: object and background. Li and Lee [6] proposed a method that minimizes the cross-entropy between the segmented and original images. Instead of maximizing, Sahoo [12] extended the criterion proposed by Kapur, minimizing the difference between the two class entropies. Cheng *et al.* [1] introduced a new criterion that involved fuzzy partitioning and the maximum entropy principle.

On the other hand, methods based on clustering address the problem as a partition problem, where the pixels/voxels of the image must be divided in two groups. One of the most popular and efficient thresholding methods in the literature, known as Otsu's Method [8], belongs to this category. This method maximizes the variance between the object and background classes. Kittler and Illingworth [5] proposed a criterion assuming that the two classes come from Gaussian density functions. Hu *et al.* [3] estimated from the image histogram the frequency ranges in which the background and the region of interest vary. Then, their method selects the threshold that minimizes the classification error within the constrained variable background range. Qiao *et al.* [11] segmented small objects by introducing knowledge about intensity contrast in their criterion function, which consists of a weighted sum of within-class variance and intensity contrast between the object and background.

In this work, we found that some of the abovementioned methods of selecting thresholds automatically fail for brain tumor segmentation. A reason for the failure may be that the methods assume low intra-class variance, or entropy, which may not be true in the case of a brain MRI. While the tumor is the object of interest, the rest of the brain tissue is the background. The brain tissue consists of different components whose intensities also vary. Therefore, the group representing voxels from the healthy tissue cannot present low intra-class variance or entropy. Furthermore, the intensity inhomogeneity present in an MRI can also affect the performance of the criterion as well as most of the segmentation methods.

We propose a new method of brain tumor segmentation that aims to preserve the simplicity and speed of thresholding. The method consists of a customized criterion for this specific problem that maximizes the contrast between the tumor and healthy region while minimizing the variance of the region of interest. The criterion also considers the sizes of the two groups, rewarding the creation of large connected components.

The method segments the regions affected by the tumor from three different types of MRIs: T2-weighted spin echo (T2), Fluid Attenuated Inversion Recovery (FLAIR), and T1-weighted after administration of a contrast medium (T1C). The differences between these MRI modalities can be seen in Figure 1. The result of the method is a binary image that masks the union of the regions segmented from the three images.

In Section 2, we explain the segmentation method and the criterion proposed in this work. In Section 3, we present the evaluation of the method for a set of images with ground truth and discuss the results. Finally, we draw some conclusions in Section 4.

2 The Segmentation Method and the Criterion

The segmentation method consists of three stages. First, some features of the image histograms are pointed out. Then, the method establishes two different intensity ranges of interest. These intensity ranges are searched for thresholds that yield the regions that we want to segment. Finally, the method applies the thresholds to the different MRI modalities to obtain a complete segmentation of the regions affected by the tumor.

2.1.Feature Point Localization in the Histogram

Before finding the thresholds that yield the tumor segmentation in the MRI modalities, the method divides the image into two sets of voxels, each with a different intensity range. This first partitioning of the image is carried out based on some feature points in the histogram. Independently of the MRI modality, a brain MRI has a characteristic shape, with at least two modes, as Figure 2 shows [2]. The first mode (μ_1) represents the image background; the second (μ_2) represents the healthy brain tissue. In addition to these two feature points, the method also localizes two more points: τa, which is the middle point between μ_1 and μ_2, that is,

$$\tau_a = \frac{\mu_1 + \mu_2}{2} \tag{2}$$

and τc, which is located at the histogram tail and is the maximum intensity value to be considered as a candidate threshold. This value applied as a threshold yields small objects whose size is less than an established minimum tumor size. Therefore, intensity values greater than τc are discarded as thresholds.

The features points, τa, μ_2, and τc, define two ranges of intensities in the histogram, as Figure 2 shows, as well as two initial sets of voxels from the image. The first set contains voxels with intensity values between τa and μ_2 and the second set contains voxels with intensity values between μ_2 and τc.

2.2.The Criterion Function for Threshold Selection

The intensity ranges defined by the feature points delimit the search space for the thresholds. In order to localize the thresholds, the method uses the criterion function introduced below.

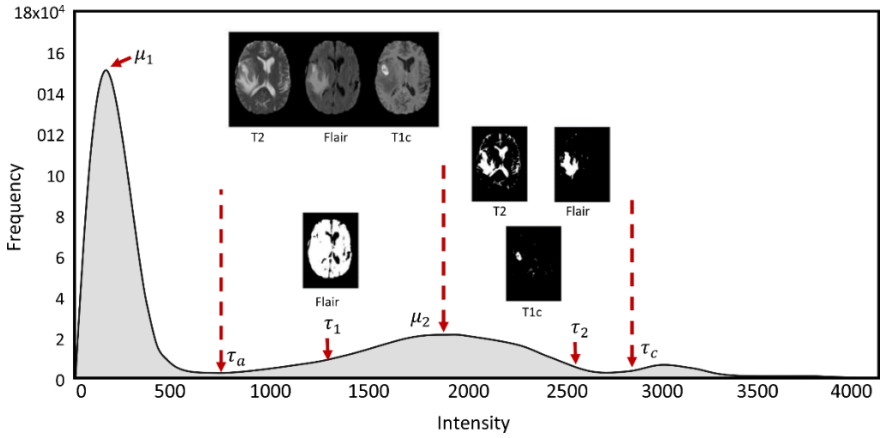

Figure 2. MRI histogram features

Let Z_L^+ be the set of intensity values present in the image $I(x, y, z)$ such that $Z_L^+ = \{i_0, i_1, \ldots, i_L\}$, where i_0 and i_L are the minimum and maximum intensity values. Let $f_{i0}, \ldots, f_{iL}$ be the intensity frequencies in the image histogram. One may estimate the percentage of a given intensity value in the image as:

$$p_i = \frac{f_i}{N}, \quad N = \sum_{i_0}^{i_L} f_i \tag{3}$$

One may divide voxels in the image $I(x, y, z)$ into two groups or classes by applying a threshold τ. This threshold also separates Z_L^+ into two ranges of intensity values. The first class C_0 will contain voxels with intensity values in the range $[i_0, \ldots, \tau]$, and C_1 will contain voxels with intensity values in the range $[\tau, \ldots, i_L]$. Table 1 shows the equations for estimating the probability of each class, the mean, and the variance. The criterion function proposed in this work to find τ is:

$$\phi(\tau) = (P_0(\mu_0 - \mu_\tau)^2)\psi_0 - (P_1\sigma_1^2)\psi_1 \tag{4}$$

where P_0 and P_1 are the probability of the classes C_0 and C_1, respectively. The variables ψ_1 and ψ_2 are the normalized sizes of the biggest connected components in both classes C_0 and C_1. The variables μ_0 and μ_T are the mean intensity values of C_0 and the complete set of voxels with intensity values in Z_L^+, and σ_1^2 is the variance of C_1. The segmentation method looks for the best threshold T^* that maximizes Equation 4, that is,

$$T^* = arg \max_{\tau = i_0, \ldots, i_L} [\phi(\tau)] \tag{5}$$

Equation 4 is a unimodal function, and therefore we used a golden section search algorithm to find the optimal threshold.

Table 1. Class probability, mean and variance equations

Class	Probability (P)	Mean (μ)	Variance(σ^2)
C_0	$P_0 = \sum_{i=i_0}^{t} p_i$	$\mu_0 = \frac{\mu(t)}{P_0}$	$\sigma_0^2 = \sum_{i=i_0}^{t} (i-\mu_0)^2 p_i / P_0$
C_1	$P_1 = \sum_{i=t+1}^{i_L} p_i$	$\mu_1 = \frac{\mu_T - \mu(t)}{1 - P_0}$	$\sigma_1^2 = \sum_{i=t+1}^{i_L} (i-\mu_1)^2 p_i / P_1$

Where $\mu_t = \sum_{i=i_0}^{t} i p_i$ and $\mu_T = \sum_{i=i_0}^{i_L} i p_i$.

2.3.Tumor Segmentation

The feature points localized in Section 2.1 are used together with Equation (4) to find a threshold τ_2 for T2 and FLAIR. The method also localizes a threshold τ_1 in FLAIR (see Figure 2). In order to localize τ_2 in T2 and FLAIR, we only take a portion of the images with voxels in the intensity range $[\mu_2, \dots, \tau_c]$ to carry out the search. Thus, the minimum and maximum values in Z_L^+ are $i_0 = \mu_2$ and $i_L = \tau_c$, respectively, for this case. The method divides this portion of the images into two classes, where the first class C_0 corresponds to the healthy tissue, with intensity values between μ_2 and τ_2. The second class C_1 contains voxels that belong to the region of interest, with intensity values greater than or equal to τ_2. The difference between the mean intensity value of the complete portion of the image and the mean value of the voxels in the class C_0 is expected to increase as the voxels corresponding to the tumor region are separated in the class C_1. Also, we expect to find that C_1 has low variance but C_0 does not. The variables ψ_1 and ψ_2 reward the segmentation of large compact regions after applying the threshold.

In the case of the threshold τ_1, Z_L^+ is taken as the set of intensity values in the range $[\tau_a, \dots, \mu_2]$. Thus, we only take a portion of the image whose voxels' intensity values fall in this range. The threshold τ_1 divides the set of voxels into two classes, where the class C_1 contains voxels in the range $[\tau_a, \dots, \tau_1)$ and class C_0 contains voxels with intensity values in the range $[\tau_1, \dots, \mu_2]$. This threshold in FLAIR segments ventricles and sulci, as shown in Figure 2.

Figure 2 also shows the resulting binary images after applying the thresholds τ_1 and τ_2 to the respective MRI modalities. The threshold τ_2 segments high intensity values, which correspond to tumor areas in the images, while the threshold τ_1 segments ventricles and sulci in FLAIR. The region of interest is easily identified in FLAIR after applying τ_2. However, it is attached to ventricles and sulci in T2. For this reason, we use the result of the threshold τ_1 to mask out the ventricles and sulci from T2 after applying τ_2. Then, the method applies morphological operations to extract connected components from the two modalities, and in this way a unique

binary image is created with a mask covering the areas affected by the tumor in T2 and FLAIR.
In order to extract the affected tumor areas from T1C, the method employs the binary mask segmented from T2 and FLAIR. Here, the method selects a set of voxels from T1C that correspond spatially to the same voxels in the binary mask. Then, the method uses Otsu's criterion (Equation 6) to separate this set of voxels belonging to the tumor into two classes.

$$\sigma_B^2(\tau) = \frac{\mu_T P_0 - \mu_0}{P_0 P_1} \tag{6}$$

The threshold used to segment the enhanced regions from T1C is the candidate that maximizes Equation 5, as Equation 7 states. Thus, voxels in the enhanced regions in the set are treated as the object and the rest of the voxels as background. Since the region covered by the mask in T1C also corresponds to tumor tissue, here we are not considering high intra-class variance for the background class.

$$\mathrm{T}^* = arg \max_{\tau = i_0, \ldots, i_L} [\sigma_B^2(\tau)] \tag{7}$$

Since the enhanced regions in T1C also appear with high intensity values, the optimal threshold found by the method is also located in the range of intensities $[\mu_2, \ldots, \tau_c]$ for this modality. Figure 3 shows a segmentation result obtained with the method described here.

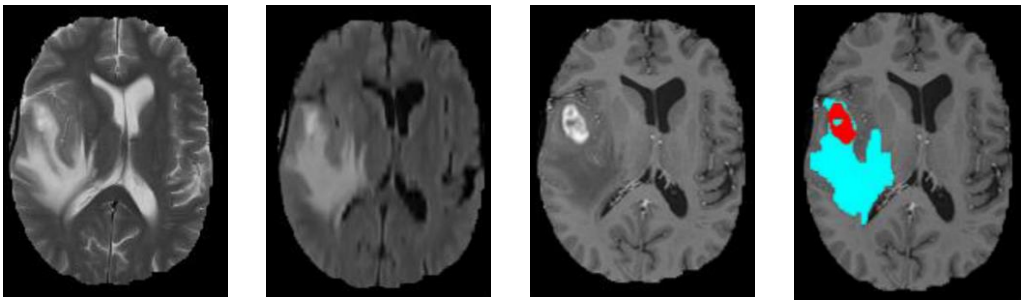

a)T2 b)Flair c)T1c d) Result

Figure 3. Result of the segmentation method. The whole region affected by the tumor in cyan and red, and the enhanced region segmented from T1C in red

3 Results

We evaluated the segmentation method on a set of images provided by the Multimodal Brain Tumor Segmentation Challenge (BRATS 2013) [7]. The set of

images consists of 30 multi-contrast MRIs of patients with low and high gliomas with and without recession. The images are co-registered between each other, skull stripped, and interpolated to an isotropic resolution of 1 mm. The set of images also contains the ground truth for each patient.
Besides the criterion for threshold selection proposed in this work, we also evaluated the method using three different criteria known in the literature: the criteria proposed by Kapur [4], Otsu [8], and Kittler [5]. Since the method's success is strongly reliant on the first mask of the tumor segmented from T2 and FLAIR, we only used the other three criteria to localize τ_2 for these two modalities.

We used the Dice coefficient as the metric for evaluating the method performance, that is, the similitude between the image segmentation by the method $M(x, y, z)$ and the manual segmentation provided by BRATS 2013 $B(x, y, z)$. Equation 7 is the metric used:

$$S_D = \frac{2a}{2a + b + c} \tag{7}$$

where S_D is a similitude coefficient between the images, a is the number of voxels that belong to the tumor and are common to *M* and B, b is the number of voxels in B that belong to the tumor but are not in *M*, and c is the number of voxels that are part of the tumor in *M* but not part of the tumor in *B*.

Equation 7 was estimated for each segmentation yielded by the method. The boxplot in Figure 4 shows the evaluation of the different criteria used for the threshold selection. Table 2 contains the means, variances, and standard deviations obtained in this experiment for each criterion.

Figure 5 shows some examples of the segmentation results obtained with the method introduced in this work using the criterion stated in Equation 5. In this figure, the obtained segmentation is represented in cyan color and the ground truth in yellow.

3.1.Discussion

As Figure 4 and Table 2 show, the segmentation method performed best with the criterion function proposed in Equation 4. The worst performance was obtained with the entropic criterion proposed by Kapur [4]. Contrary to the criterion proposed in this work, the other criteria yielded thresholds out of the search ranges in Figure 2, sub-segmenting the regions of interest. Table 3 summarizes the number of cases in which the thresholds failed to produce any segmentation because they were high intensity values.

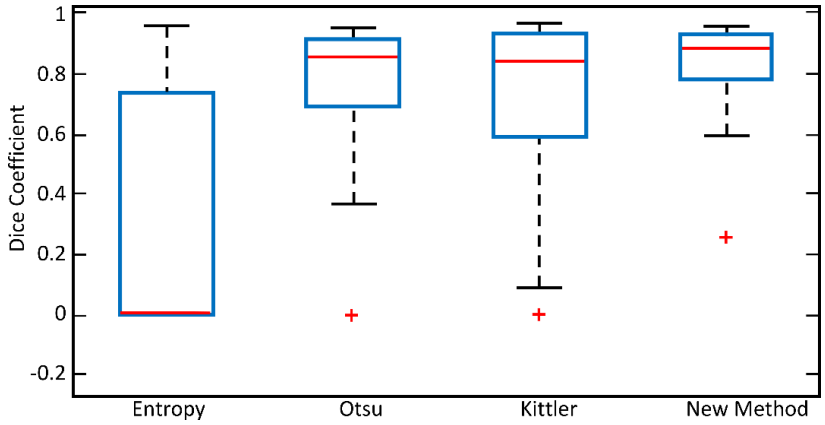

Figure 4. Box plot of Dice coefficients of the method with different criterion functions for threshold localization

Table 2. Mean, variance and standard deviation of each criterion evaluated over the set of images provided by BRATS 2013

Criterion function	Mean	Variance	Standard deviation
Entropic	0.33	0.14	0.38
Otsu	0.75	0.04	0.21
Kittler	0.66	0.12	0.34
New criterion	0.81	0.02	0.14

Table 3. Amount of failed cases by criterion function

Criterion function	Number of failed cases
Entropic	16
Otsu	1
Kittler	5
New criterion	0

The entropic criterion function failed in more than half of the cases, which can be a reason for the low mean value in Table 2. The Otsu and new criteria gave the lowest variance of the experiment, while the Kittler criterion gave the highest variance, which indicates that its performance differed between most of the cases.

The segmentation method with the new criterion was fast, taking around one minute per case, and simple to use since it did not require any complex input. The method also performed fast with the Otsu and Kittler criteria, but took more than one minute per case using the entropic criterion.

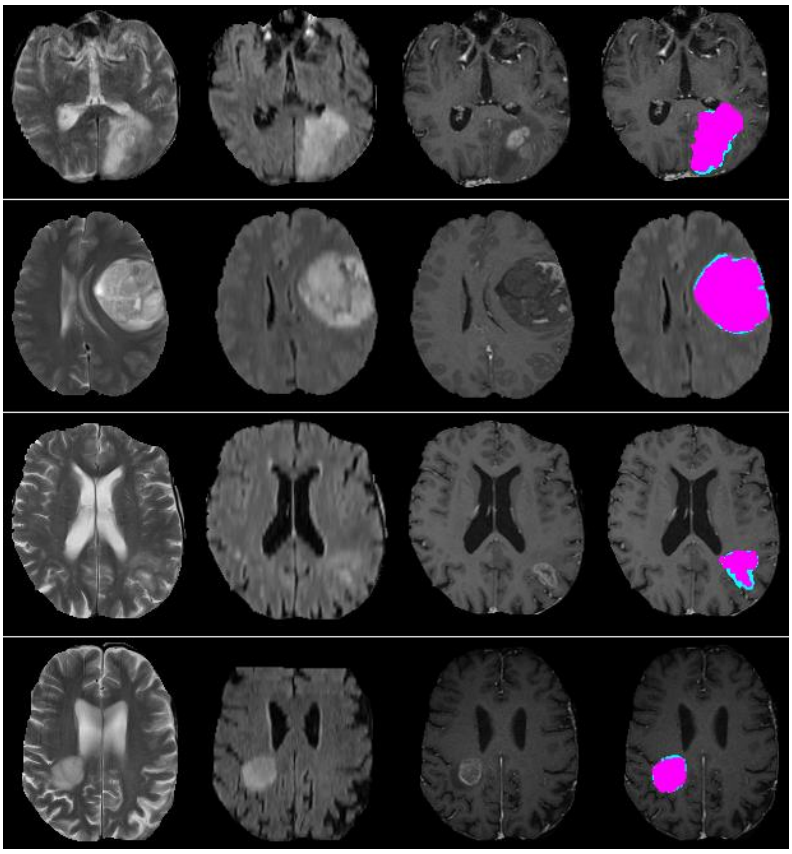

Figure 5. Segmentation Results. From top to bottom four different tumor cases with their respective three MRI types; T2, Flair and T1c. The last image of each row is the method's result in magenta over the ground truth in cyan

4 Conclusion

In this work, we introduced a novel brain tumor segmentation method with a new criterion function for automatic threshold selection. This new criterion function can be seen as an extension of Otsu's criterion without assuming low intra-class variance for both classes, and involving the size of the compact objects segmented by the threshold. In this way, the new criterion function is specialized in separating healthy tissue from the tumor. The first term of the function aims to segment large connected components whose mean values differ with respect to the whole image, as voxels with high intensities are grouped in another class. The second term aims to generate a compact segmented region whose variance should be low, corresponding to the tumor.

We evaluated the performance of the method on a set of images provided for the segmentation challenge presented in [7] and compared the criterion function with other criterion functions that are well-known in the literature for automatic threshold selection. The new criterion outperformed the other three criteria, which

were the functions proposed in [4], [5], and [8]. The method segments the regions affected by the tumor in three modalities, and the result is a binary image with the union of the three outcomes. This mask can be used to design a more sophisticated method to further segment the tumor into its components: edema, enhanced core, cysts, and so on.

References

H.D. Cheng, J.-R. Chen and J. Li, Threshold selection based on fuzzy c-partition entropy approach, *Pattern Recognition*, **31** (1998), no. 7, 857-870.

[2] I. Diaz, P. Boulanger, R. Greiner, B. Hoehn, L. Rowe, and A. Murtha, An automatic brain tumor segmentation tool, *2013 35th Annual International Conference of the IEEE Engineering in Medicine and Biology Society (EMBC)*, (2013), 3339-3342. http://dx.doi.org/10.1109/embc.2013.6610256

[3] Q. Hu, Z. Hou, and W.L. Nowinski, Supervised range-constrained thresholding, *IEEE Transactions on Image Processing*, **15** (2006), no. 1, 228-240. http://dx.doi.org/10.1109/tip.2005.860348

[4] J.N. Kapur, P.K. Sahoo and A.K.C. Wong, A new method for gray-level picture thresholding using the entropy of the histogram, *Computer Vision, Graphics, and Image Processing*, **29** (1985), no. 3, 273-285. http://dx.doi.org/10.1016/0734-189x(85)90125-2

[5] J. Kittler and J. Illingworth, Minimum error thresholding, *Pattern Recognition*, **19** (1986), no. 1, 41-47. http://dx.doi.org/10.1016/0031-3203(86)90030-0

[6] C.H. Li and C.K. Lee, Minimum cross entropy thresholding, *Pattern Recognition*, **26** (1993), no. 4, 617-625. http://dx.doi.org/10.1016/0031-3203(93)90115-d

[7] B.H. Menze and et al., The Multimodal Brain Tumor Image Segmentation Benchmark (BRATS), *IEEE Transactions on Medical Imaging*, **34** (2015), no. 10, 1993-2024. http://dx.doi.org/10.1109/tmi.2014.2377694

[8] N. Otsu, A Threshold Selection Method from Gray-Level Histograms, *IEEE Transactions on Systems, Man, and Cybernetics*, **9** (1979), no. 1, 62-66. http://dx.doi.org/10.1109/tsmc.1979.4310076

[9] E. Prieto, P. Lecumberri, M. Pagola, M. Gómez, I. Bilbao, M. Ecay, I. Peñuelas and J.M. Martí-Climent, Twelve automated thresholding methods for segmentation of PET images: a phantom study, *Physics in Medicine and Biology*, **57** (2012), no. 12, 3963-3980.

http://dx.doi.org/10.1088/0031-9155/57/12/3963

[10] T. Pun, A new method for grey-level picture thresholding using the entropy of the histogram, *Signal Processing*, **2** (1980), no. 3, 223-237. http://dx.doi.org/10.1016/0165-1684(80)90020-1

[11] Y. Qiao, Q. Hu, G. Qian, S. Luo and W.L. Nowinski, Thresholding based on variance and intensity contrast, *Pattern Recognition*, **40** (2007), no. 2, 596-608. http://dx.doi.org/10.1016/j.patcog.2006.04.027

[12] P. Sahoo, C. Wilkins and J. Yeager, Threshold selection using Renyi's entropy. *Pattern Recognition*, **30** (1997), no. 1, 71-84. http://dx.doi.org/10.1016/s0031-3203(96)00065-9

Received: June 3, 2016; Published: July 15, 2016